Julio A. Deiber[1]
Maria V. Piaggio[2]
Marta B. Peirotti[1]

[1]Instituto de Desarrollo Tecnológico para la Industria Química (INTEC), Universidad Nacional del Litoral (UNL), Consejo Nacional de Investigaciones Científicas y Técnicas (CONICET), Santa Fe, Argentina
[2]Cátedra de Bioquímica Básica de Macromoléculas, Facultad de Bioquímica y Ciencias Biológicas, UNL, Santa Fe, Argentina

Received May 18, 2014
Revised June 11, 2014
Accepted June 16, 2014

Research Article

Estimation of electrokinetic and hydrodynamic global properties of relevant amyloid-beta peptides through the modeling of their effective electrophoretic mobilities and analysis of their propensities to aggregation†

Neuronal activity loss may be due to toxicity caused by amyloid-beta peptides forming soluble oligomers. Here amyloid-beta peptides (1–42, 1–40, 1–39, 1–38, and 1–37) are characterized through the modeling of their experimental effective electrophoretic mobilities determined by a capillary zone electrophoresis method as reported in the literature. The resulting electrokinetic and hydrodynamic global properties are used to evaluate amyloid-beta peptide propensities to aggregation through pair particles interaction potentials and Brownian aggregation kinetic theories. Two background electrolytes are considered at 25°C, one for pH 9 and ionic strength $I = 40$ mM (aggregation is inhibited through NH_4OH) the other for pH 10 and $I = 100$ mM (without NH_4OH). Physical explanations of peptide oligomerization mechanisms are provided. The effect of hydration, electrostatic, and dispersion forces in the amyloidogenic process of amyloid-beta peptides (1–40 and 1–42) are quantitatively presented. The interplay among effective charge number, hydration, and conformation of chains is described. It is shown that amyloid-beta peptides (1–40 and 1–42) at pH 10, $I =$ 100 mM and 25°C, may form soluble oligomers, mainly of order 2 and 4, after an incubation of 48 h, which at higher times evolve and end up in complex structures (protofibrils and fibrils) found in plaques associated with Alzheimer's disease.

Keywords: Aggregation rates / Amyloid-beta / Electrokinetic properties / Electrophoretic mobility / Hydrodynamic properties
DOI 10.1002/jssc.201400533

Additional supporting information may be found in the online version of this article at the publisher's web-site

1 Introduction

CZE is a powerful analytical method [1–6] to characterize the electrokinetic and hydrodynamic global properties of complex polyampholyte-polypeptide heterochains through the modeling of their effective electrophoretic mobilities in BGEs with well defined temperature, pH, ionic strength I, electrical permittivity ε, and viscosity η_s [7–29]. Chain properties are then needed to find out relevant biophysical mechanisms describing biological systems. In this regard, proteins and peptides may be studied in different BGEs formulated to pursue biological subjects, where bioprocesses involved in human pathologies and associated biomarkers still require elucidation to incur in a trial clinical stage. Within this framework a typical specific case is Alzheimer's disease (AD), for which a definite etiopathology is not well known at present. Several hypotheses have been proposed, and among them, the loss of neuronal activity due to toxicity caused by amyloid-beta (Aβ) peptides forming soluble aggregates is considered one of the most probable. In fact the histopathology is characterized by extracellular plaques formation caused by aggregation of mainly Aβ(1–42) with an amino acid sequence (AAS) DAEFRHDSGYEVHHQKLVFFAEDVGSNKGAIIGLMVGGVVIA, and Aβ(1–40) where the terminal I(41) and A(42) are not present. In this regard, the "amyloid cascade hypothesis" [30, 31] establishes that the initiation of AD involves the accumulation of main Aβ peptides

Correspondence: Dr. Julio A. Deiber, INTEC, Güemes 3450, 3000, Santa Fe, Argentina
E-mail: treoflu@santafe-conicet.gov.ar
Fax: +54-(0)342-4550944

Abbreviations: **AAS**, amino acid sequence; **Aβ**, amyloid-beta; **AD**, Alzheimer's disease; **DLVO**, Derjaguin–Landau–Verwey-Overbeek; **PPIP**, pair particles interaction potential

†This paper is included in the virtual special issue on Amino acids, proteins and peptides available at the Journal of Separation Science website.

as a consequence of an imbalance between their production and clearance. From both familial and sporadic AD, the result is an increase in Aβ soluble oligomers, intermediates, and fibrils with a progressive formation of amyloid plaques, where the addition of new aggregates occurs. Also the kinase/phosphatase activity is altered resulting neurofibrillary tangle formations via high hyperphosphorilated tau protein provoking disruption of axonal transmission [30–32]. Therefore, neuronal and synaptic dysfunction takes place. Another biophysical aspect considered is that some Aβ peptides suffer a conformational change favoring the aggregation into soluble oligomers [33]. Several other causes and effects promoting or inhibiting Aβ peptides aggregation need to be elucidated [30–32, 34]. In general the specific molecular mechanisms yielding extracellular plaques are not well understood yet.

From the basic point of view, in the amyloidogenic pathway [30, 31] the intramembrane amyloid precursor protein (APP) is cleaved through the beta-secretase to release a part of the soluble extracellular domain into the plasma and cerebrospinal fluid. Then the carboxy-terminal fragment of APP that remains in the plasma and membrane is cleaved through the γ-secretase system, composed of four enzymes, thus generating Aβ(1–42) and its carboxy-truncated isoforms Aβ(1–17) to Aβ(1–40). Further the α-secretase generates the other known peptides fragments from Aβ(1–13) to Aβ(1–16).

In the search of biophysical mechanisms and biomarkers associated with AD, the following five peptides were electrokinetically and hydrodynamically characterized here: Aβ(1–37) to Aβ(1–40) and Aβ(1–42), which were studied by CZE–UV in Ref. [35]. These global properties are then useful to evaluate Aβ peptide propensities to aggregation when attention is focused into the basic pair particles interaction potentials (PPIPs) and aggregation kinetics theories. The effect of initial peptide molar concentration C_p on the aggregation mechanisms is also important from the thermodynamic and kinetic points of view.

The biophysical mechanisms leading to Aβ(1–40) and Aβ(1–42) aggregations may be targeted from two basic scales. One considers details of peptide primary configuration and structure described by the AAS and the physicochemical characteristics and roles of each type of amino acid residue ([36–38] and citations therein), while the other is concerned with peptide chain global properties and conformations associated with hydrodynamic and electrokinetic effects enhancing peptides aggregation [35, 39–44]. In the consideration of this last scale, CZE methods may assist one significantly to understand some of the basic mechanisms of Aβ peptides aggregation at different incubation times t_i by providing particle migration times t_m associated with the detection of monomer and soluble oligomer peaks. Despite the fact that these evaluations may be processed and modeled to arrive at relevant conclusions concerning AD, the CZE method has not been exploited enough for these purposes, as one may judge from the relatively few works [35, 39–44] dedicated to this specific application ([45] and citations therein).

This work presents the evaluation of global properties of the five Aβ peptides having $N = 37$, 38, 39, 40, and 42 amino acid residues through the modeling of their effective electrophoretic mobility obtained by CZE–UV as provided in Ref. [35]. One protocol of this work, where chain aggregation was inhibited, allowed us the characterization of these peptides individually. Following another protocol of this work we studied the propensity to aggregation of Aβ(1–42) and Aβ(1–40) by using their global properties and well established kinetic theories of Brownian aggregation [46,47]. For these purposes, the perturbed Linderstrøm–Lang CE model was used by taking into account that its applicability to polyampholyte-polypeptide chains has been discussed in detail in Refs. [8, 12, 13, 15, 17, 18, 20, 22, 25–29] pointing out the approximations introduced (see also some details in the Supporting Information). From the framework of spherical and aspherical particles we provide here relevant electrokinetic and hydrodynamic properties of the five Aβ peptides and the characteristic rapid and slow doublet formation kinetic constants of peptide Brownian aggregation.

2 Materials and methods

2.1 Peptide samples and CZE–UV protocols

The experimental information concerning the five Aβ peptides was extracted from Ref. [35] where solutions with peptide concentration 0.033 mg/mL were prepared to assure solubility. To avoid peptide aggregation via β-sheet formation, mainly of Aβ(1–42) and Aβ(1–40), 0.004% m/v of NH_4OH was added. Methods for peptide dissolution and solution storage at −20°C are well described in Ref. [35]. A small amount (3 mM) of 1,4-diaminobutane was also added in the BGE to control the EOF, thus permitting a neat electrophoretic separation of the five peptides. This amount had a minor effect on the peptide's effective electrophoretic mobility as discussed by the authors in their optimization procedure. The protocol selected for the separation of the five peptides was pH 9, $I = 40$ mM in borate buffer at 25°C. Values of t_m were obtained here to estimate the effective electrophoretic mobility μ_p^{exp} of the five peptides. When another protocol with pH 10, $I = 100$ mM in borate buffer and without the aggregation inhibitor was used, the sample incubation time t_i became an important parameter. In fact estimated calculations from UV-absorbance ratios indicated that the peptide mass concentration of Aβ(1–42) changed initially from 0.033 to around 0.007 mg/mL at 48 h, while the aggregation was lower for Aβ(1–40) in the same time with a change from 0.033 to around 0.018 mg/mL. Therefore, this relevant information allowed us to consider also the amyloidogenic pathway of these two Aβ peptides in this specific BGE by considering the theoretical framework described briefly in Section 2.2.3. In this regard, global properties and propensities to aggregation of Aβ(1–40) and Aβ(1–42) were evaluated as a first step toward future studies on this subject via the CZE–UV method.

2.2 Theoretical concepts and considerations

2.2.1 Electrokinetic and hydrodynamic global properties

The electrokinetic and hydrodynamic peptide global properties estimated here are ([8, 18, 20, 22, 25, 28, 29] and Supporting Information): effective electrical charge number Z, total electrical charge number Z_T, effective charge number fraction $\Delta\sigma = |Z|/N$, total charge number fraction $\sigma = Z_T/N$, approximate hydration designated H (number of water molecules per chain) or δ (gram of water/gram of peptide), size estimated via the hydrated equivalent hydrodynamic Stokes radius a_H, compact radius a_c accounting for the chain mass only, packing fractal dimension g_p, friction fractal dimension g_f, friction ratio Ω (also designated asphericity) where both the stick and slip between fluid and hydrated particle may be considered [28], pH of the chain microenvironment designated pH* due to particle charge regulation phenomenon, average peptide specific volume v_p [18]. The characterization of the monomer state of peptides through these global properties is relevant taking into account that for high enough incubation times of their soluble oligomers, Aβ peptides may evolve ending up in complex structures like protofibrils and fibrils typically found in AD [45].

2.2.2 Maximum and minimum peptide hydration

Peptide hydration is here defined $H = H_o + H_d$, where H_o is the number of water molecules captured by amino acid residues of peptide AAS, while H_d is the number of water molecules due to the degree of water occlusion or release by peptides (see Supporting Information and details in Ref. [18]). It is clear that H is dependent in part on the AAS and protocol pH [28, 29]. An important physical interplay between particle shape and hydration is that for a given μ_p^{exp} involving either peptides and proteins, $H_d = 0$ and $\Omega < 1$ implies the minimum δ value sampled by the chain, while the same μ_p^{exp} with $H_d > 0$ and $\Omega = 1$ gives the maximum hydration value physically admissible as demonstrated and validated previously [12, 13, 18, 28]. Conversely, when a given μ_p^{exp} yields $\Omega > 1$ with $H_d = 0$ for both spherical and aspherical hydrated particles (BGE slip or stick at these particle surfaces may apply, respectively [28]). $H_d < 0$ is required to obtain $\Omega = 1$ giving a minimum hydration as long $a_H \geq a_c$ is satisfied [12, 28]. Some peptide conformations sampled as spherical particles cannot give a solution in this last case because unphysical results are obtained when $a_H < a_c$.

2.2.3 Pair particles interaction potentials and Brownian kinetics of aggregation

CZE–UV is a powerful method to study experimentally different conformational states, like those found in the protein native-unfolding problem [13, 48] and the propensity to aggregation of interacting polypeptide chains, at appropriate concentrations and BGE formulations. Concerning the later application, the understanding of global forces intervening in the oligomerization of interacting hydrated particles (here hydrated polyampholyte–polypeptides chains) is still a subject of research with many aspects to be elucidated yet, as discussed in the literature ([47, 49] and citations therein). Nevertheless, at present there is available a theoretical framework providing relevant mechanisms which may be applicable to the amyloidogenic process of peptides when some electrokinetic and hydrodynamic global properties values are obtained. For the purposes of this work we consider three basic forces that control the oligomerization of Aβ peptides. First it is appropriate to quantify electrostatic repulsion and dispersion attractive forces associated with the Derjaguin–Landau–Verwey–Overbeek (DLVO) theory [50, 51]. These forces require values of electrokinetic and hydrodynamic global properties obtained from CZE–UV (Sections 2.2.1 and 2.2.2). Thus a simple expression for the repulsion electrostatic PPIP designated U_R between two particles as a function of the distance r between their centers is [47]

$$U_R \approx 32\pi\varepsilon \left(\frac{k_B T}{e}\right)^2 a_H \tanh^2\left(\frac{e\zeta}{k_B T}\right) \exp(-\kappa(r - 2a_H)) \quad (1)$$

where e is the elementary charge, $\zeta = eZ/(4\pi\varepsilon a_H(1 + \kappa a_H))$ is the peptide zeta (electrokinetic) potential, $\kappa = (2Ie^2 N_A 10^3/\varepsilon k_B T)^{1/2}$ is the Debye–Hückel parameter, k_B is the Boltzmann constant, T is the absolute temperature and N_A is the Avogadro constant. The attractive dispersion PPIP designated U_A is [47]

$$U_A \approx -\frac{1}{6} A_H^{eff}(r - 2a_H)\left(\frac{2a_H^2}{r^2 - 4a_H^2} + \frac{2a_H^2}{r^2} + \ln\frac{r^2 - 4a_H^2}{r^2}\right) \quad (2)$$

where $A_H^{eff}(r - 2a_H)$ is the effective Hamaker function depending on r when UV relaxations dominating part of the dielectric spectra are considered. When relaxation effects are neglected A_H^{eff} becomes the classical Hamaker constant A_H as defined and evaluated in the Supporting Information, giving for these peptides around 1.51×10^{-20} J. These two DLVO forces are relevant for pair particle distances in the range 1–5 nm. They do not apply when particles become near contact. Additional hypotheses concerning Eqs. (1) and (2) are well described in Ref. [47] and citations therein. When hydration is relevant in these particles, the consideration of the hydration force in aqueous solutions is appropriate, which is included in the framework of the non-DLVO theory. Typically the following empirical equation for the repulsive hydration PPIP designated U_H may be used ([49] and citations therein),

$$U_H \approx \pi a_H L_H \Delta G \exp(-(r - 2a_H)/L_H) \quad (3)$$

In Eq. (3), L_H is the structural water layer around the hydrated particle. Therefore, we also found appropriate to express $L_H \approx N_L(a_H - a_c)$ as the product of the number of structural water layers N_L of hydration thickness $(a_H - a_c)$. Here ΔG is interpreted as the free energy per unit surface

area associated with water molecules interchange between bulk BGE and structural water layer when $r \to 2a_H$. For numerical calculations involving Eq(3). one must visualize that for a given value U_H, a decrease in ΔG requires higher values of L_H, and $L_H \leq 1/\kappa$ is also approximately expected. To consider Eqs. (1) to (3) as a first approximation to study the aggregation of peptides assumed as hydrated polyampholyte-polypeptide particles with weak ionizing groups, we also add here the restriction that the "pair particle charge regulation phenomenon" is neglected as a first approximation. In fact, PPIPs may present additional phenomenological coupling effects at close distances, and hence data of the effective electrophoretic mobility of both peptide monomers and oligomers are required as those reported, for instance, in Ref. [43].

From Eqs. (1) to (3), the aggregation stability ratio $W = k_r/k_s$ can be estimated where $k_r = 16\pi a_H D$ is the rapid doublet formation kinetic constant when peptide diffusion is controlling the aggregation. On the other hand when a potential repulsive barrier is the controlling mechanisms the slow doublet formation kinetic constant is [47]

$$k_s = 8\pi D \Big/ \int_{2a_H+\Delta}^{\infty} \exp(U/k_B T) dr/r^2 \quad (4)$$

where the peptide diffusion coefficient $D = \Omega k_B T/(6\pi\eta_s a_H)$ is evaluated as proposed in Ref. [18]. Also, $\Delta \approx 0.1$ nm [47] and the total PPIP is $U = U_R + U_A + U_H$ giving a total pair particle interacting force $F = -\partial U/\partial r$. Thus $k_s << k_r$ when a positive maximum of $U(r)$ is found and hence an appropriate dimensionless repulsion barrier $U_{max}/k_B T >> 1$ may be defined. Then from the classical Smoluchowski aggregation theory [46] the number of aggregates $n_k(t)$ with k monomers or disaggregated Aβ peptides, at incubation time t_i is expressed, $n_k(t_i)/n_o = (t_i/\tau)^{k-1}/(1 + t_i/\tau)^{k+1}$, where the initial number concentration of monomer is $n_o = 10^3 C_p N_A/M$ and $\tau = 3\eta_s W/(4n_o k_B T\Omega)$ (calculations use unit of h for τ) is the characteristic aggregation time. Here M is the monomer molar mass. Also $n_1(0) = n_o$ and $n_k(0) = 0$ for $k > 1$ indicating that at $t_i = 0$ the solution contains monomers only. This theory considers: (i) W is independent of aggregate sizes and (ii) the most probable aggregations occur between pairs of particles of equal size. Further details of our calculation scheme with this theory are presented in the Supporting Information.

3 Results and discussion

Table 1 shows numerical results of the five peptides electrokinetic and hydrodynamic global properties when the minimum hydration state of the aspherical particle is considered ($H_d = 0$ and $\Omega < 1$). Some global properties may vary from around 5 to 10% when Aβ(1–37) and Aβ(1–42) are compared. Thus hydration δ is around 5% higher for Aβ(1–37) than for Aβ(1–42), indicating a major repulsion in the former peptide due to the resulting hydration force [Eq. (3)], which is consistent with numerous previous findings indicating that Aβ(1–42) is the most aggregating one. Also zeta electrical potentials show a difference of the order of 4% in favor of a higher electrostatic repulsion force [Eq. (1)] among Aβ(1–37) chains, as expected from previous results, indicating that increasing the concentration C_p (closer approach between particles) Aβ(1–42) will have a lower pair electrostatic repulsion force than Aβ(1–37). This last situation favors the onset of oligomerization for Aβ(1–42). It is relevant that the friction ratio of Aβ(1–37) is around 10% higher than that of

Table 1. Numerical results of hydrodynamic and electrokinetic global properties of Aβ(1–37) to Aβ(1–40) and Aβ(1–42) peptides for pH 9, I = 40 mM and 25°C. The model considers aspherical particles (Ω < 1) with minimum hydration (H_d =0). BGE stick boundary condition applies. These peptides have p*I* ≈5.44

Peptides	Aβ(1–37)	Aβ(1–38)	Aβ(1–39)	Aβ(1–40)	Aβ(1–42)
$\mu_p^{exp} \times 10^8$ ($m^2V^{-1}s^{-1}$)	−1.510	−1.527	−1.554	−1.575	−1.604
$a_H \times 10^{10}$ (m)	12.23	12.27	12.36	12.45	12.61
M $\times 10^3$ (kg/mol)	4070	4127	4226	4325	4509
$v_p \times 10^3$ (m^3/kg)	0.701	0.700	0.702	0.705	0.710
$a_c \times 10^{10}$ (m)	10.42	10.45	10.55	10.65	10.82
pH*	8.44	8.45	8.45	8.46	8.47
Z	−3.96	−3.96	−3.97	−3.97	−3.97
δ	0.433	0.431	0.425	0.420	0.412
H	98	99	100	101	103
ζ (mV)	−32.86	−32.70	−32.39	−32.08	−31.51
Ω	0.862	0.876	0.900	0.921	0.954
g_p	2.486	2.488	2.495	2.502	2.511
g_f	0.443	0.438	0.429	0.422	0.411
σ	0.275	0.267	0.261	0.254	0.242
Δσ	0.107	0.104	0.102	0.099	0.095
AHI[a)]	−1.02	−1.05	−0.92	−0.80	−0.58

a) Average hydrophobic index: AHI; Maximum AHI = 10 and minimum AHI = −10.

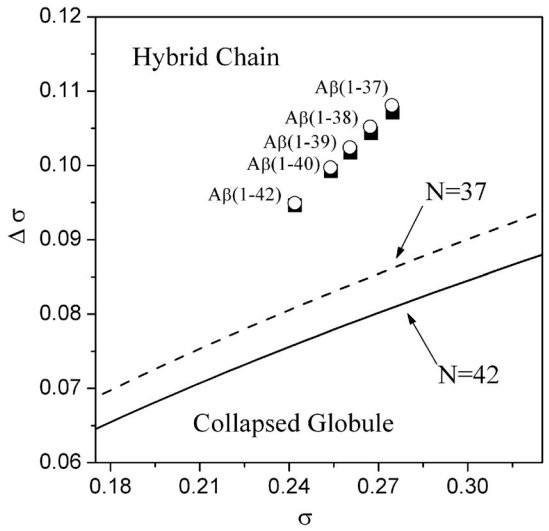

Figure 1. Effective charge number fraction $\Delta\sigma = |Z| / N$ as a function of total charge number fraction $\sigma = Z_T/N$ of Aβ(1–37) to Aβ(1–40) and Aβ(1–42) peptides. Dashed and full lines indicate the transition zone between hybrid chain and collapsed globule regimes described through $\Delta\sigma = (\sigma/N)^{1/2}$ for $N = 37$ and 42. Symbols ■ and ○ refer to calculations with aspherical and spherical particles, respectively.

Aβ(1–42). This is physically consistent with the value $g_f = 0.443$ for Aβ(1–37) presenting a more open conformation nearer to theta-condition [18, 20, 22, 25, 28, 29] than Aβ(1–42) with $g_f = 0.411$, which is approaching the collapse globule regime (Fig. 1). All these results seem to be consistent in relation to calculations showing that Aβ(1–42) is also the most hydrophobic of the five peptides. In fact, the evaluation of the average hydrophobic index [29] indicates that Aβ(1–42) is more hydrophobic in around 43% than Aβ(1–37) (Table 1). It is important to point out that the repulsion PPIP due to hydration is enhanced with the hydrophilic nature of particle surfaces [49].

From Table 1 similar qualitative comparisons as those carried out above for Aβ(1–37) and Aβ(1–42) may be performed between Aβ(1–40) and Aβ(1–42) reaching the conclusion that the former has less propensity to aggregation than the later as already reported experimentally in a high number of citations. In particular, Aβ(1–42) is 28% more hydrophobic than Aβ(1–40), which also takes a role in the amyloidogenic process through the hydration PPIP [Eq. (3)].

Table S1 of the Supporting Information shows numerical results of the five peptides global properties when the maximum hydration state of the spherical particle is considered ($H_d \neq 0$ and $\Omega = 1$). Thus for instantaneous conformations incorporating water and yielding a particle with spherical shape and relatively low surface forces, one finds that the hydration of Aβ(1–42) is much lower than that of Aβ(1–37) in around 39%. This is a strong evidence that in the random approach between high hydrated pair of Aβ(1–42) chains at an appropriate C_p value (relatively low distance between particles) the hydration repulsive force obtained from Eq. (3) is relatively lower, thus creating favorable conditions for nucleation and aggregation. It must be added to this physical situation the fact that electrostatic repulsion derived from Eq. (1) is also lower for this peptide (Supporting Information Table S1). This analysis shows that the probability to aggregate is higher for Aβ(1–42) than for Aβ(1–37).

Table 2. Numerical results from the study of propensity to aggregation of Aβ(1–40) and Aβ(1–42) peptides at pH 10, I =100 mM and 25°C, for $\Delta G \approx 32$ mJ/m^2. The model considers spherical particles with maximum hydration (Ω =1 and $H_d \neq 0$). BGE stick boundary condition applies. Also t_i =48 h and A_H =1.51 $\times 10^{-20}$ J

Peptides	Aβ(1–40)	Aβ(1–42)
U_{max}/k_BT	28	26
τ (h)	134.21	36.27
$L_H \times 10^{10}$ (m)	9.90	9.57
N_L	4.14	4.69
$D \times 10^{10}$ (m^2/s)	1.85	1.88
$k_r \times 10^{17}$ (m^3/s)	1.22	1.22
$k_s \times 10^{27}$ (m^3/s)	0.90	3.48
$W \times 10^{-9}$	13.48	3.49

Figure 1 shows the conformational evolution line of $\Delta\sigma$ versus σ [22,29] corresponding to the five peptides at pH 9, I = 40 mM and at 25°C. These peptides are close to the transition zone from the hybrid chain to the collapsed globule regimes, and from Aβ(1–37) to Aβ(1–42) conformational states tend to the collapsed regime The fact that the BGE at pH 9 used for separation purposes in Ref. [35] did not allow peptide aggregation for $t_i < 24$ h shows that the characterization of each peptide individually is in addition useful to analyze the role of global forces in the amyloidogenic process where electrostatic and hydration repulsion and dispersion attractive forces are involved, at least in qualitative terms [47, 49].

Although from Table 1 and Supporting Information Table S1 one observes that the five Aβ peptides studied here did not present significant differences in electrokinetic and hydrodynamic global properties evaluated at pH 9 and I = 40 mM, it is worth to take into account however that subtle variations detected and discussed above of the monomer Aβ peptides are significantly affecting their Brownian aggregation kinetics when quantitative estimations are carried out in the framework of Smoluchowski theory described at the end of Section 2.2.3. In fact this quantitative analysis is possible when the protocol at pH 10, I = 100 mM and the change of C_p after incubation of 48 h are considered for Aβ(1–40) and Aβ(1–42). In this regard, Supporting Information Tables S2 and S3 provide electrokinetic and hydrodynamic global properties for these peptides obtained from the theory described in Sections 2.2.1 and 2.2.2, so that they can be used in Section 2.2.3 to evaluate the aggregation kinetic parameters reported in Table 2 and Supporting Information Table S4 for spherical (maximum hydration) and aspherical (minimum hydration) through the numerical procedure described briefly in the Supporting Information. In this regard, Table 2 validates

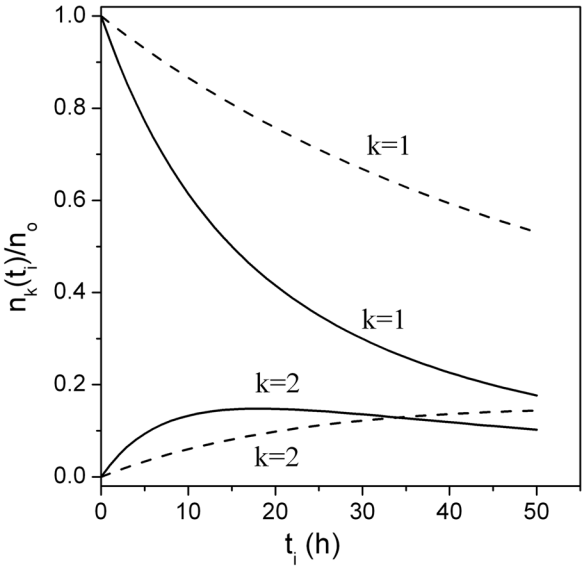

Figure 2. Prediction of peptide aggregation fractions $n_k(t)/n_o$ for $k = 1$ and 2 monomers as a function of incubation time t_i. Dashed and full lines refer to Aβ(1–40) and Aβ(1–42), respectively.

the qualitative discussion presented above. In fact we found that in the state of maximum hydration at pH 10, $I = 100$ mM and 25°C, Aβ(1–42) has a higher propensity to aggregate than Aβ(1–40) due to the following relative physical considerations concerning the former peptide: (i) the repulsion hydration force is lower due to lower values of hydration layer L_H, (ii) the slow kinetic rate k_s is higher by one order of magnitude, which is also reflected in the stability ratio W, despite the rapid doublet formation kinetic constants of these Aβ peptides are near equal as expected, because their diffusion coefficients involve similar molar masses (their AASs differ in two amino acid residues only). Here $\Delta G \approx 32$ mJ/m^2 has been used for numerical calculations reported in Table 2 and Supporting Information Table S4 mainly taking into account that the controlling parameter concerning the validation under analysis satisfies $L_H \leq 1/\kappa$, as obtained from numerical calculations when the incubation time is $t_i = 48$ h and $C_p(t_i)$ are the input experimental data. Monomer concentrations at this incubation time are illustrated in Fig. 2 for spherical particles. This figure also shows that at 48 h, Aβ(1–42), and Aβ(1–40) present dimer fraction values 0.102 and 0.144, respectively. For $k = 2$, this figure shows that full and dashed lines are crossing one another indicating consistently that the maximum value of dimer formation for Aβ(1–42) occurs earlier (at around 18 h) than that of Aβ(1–40) (at around 67 h). Tetramer fractions not shown in Fig. 2 are 0.034 and 0.011 for Aβ(1–42) and Aβ(1–40), respectively. Higher order oligomer fractions take values $< 10^{-3}$ but still high enough for the onset of a slow amiloydogenic process, of course considering that input data come from an experimental study in vitro.

For the state of minimum hydration at pH 10, $I = 100$ mM and 25°C (Supporting Information Table S4), the same validation and conclusions are obtained for the relative propensities to aggregate of Aβ(1–40) and Aβ(1–42). Also it is relevant to visualize from Table 2 and Supporting Information Table S4 that while L_H still plays the same role in both situations of maximum and minimum particle hydrations, the relative values of the number of hydration layers N_L becomes lower for Aβ(1–40) than for Aβ(1–42) when $\Omega = 1$ because the layer thickness $(a_H - a_c)$ of Aβ(1–40) increases significantly (see Supporting Information Tables S2 and S3 and the text below Eq. (3)). In fact, this particle hydration is high and N_L tends to be lower because a_H becomes also high giving $a_H >> a_c$.

Finally, the analysis of each PPIP contribution to the resultant peptide aggregation rates indicates that the repulsive hydration force is relatively significant when the peptide stability ratio estimated from experimental data are fitted by Eqs. (1) to (3) and the aggregation Smoluchowski theory. In this regard, this theoretical framework should be improved by considering, for instance, the "pair particle charge regulation phenomenon" at very short separating distances between particles. This additional effect may be added to the "self charge regulation phenomenon" of the particle alone already considered here.

4 Concluding remarks

Electrokinetic and hydrodynamic properties of Aβ peptides evaluated from the modeling of their effective electrophoretic mobilities at well defined BGE properties are required to estimate the propensity to aggregation of these polyampholyte-polypeptide chains having weak ionizing groups. It was also shown that CZE–UV is one of the most appropriate experimental methods for the following purposes: (i) to obtain peptide monomer concentration ratios at different incubation times and (ii) to achieve the evaluation of a well defined set of global properties needed in calculations involving Brownian aggregation theories. These theories are able to estimate values of the Aβ peptide stability ratio and the slow aggregation kinetic rate. Our forthcoming work will consider the effects of Aβ peptide concentration, aggregate sizes, and "pair particle charge regulation phenomenon" on the amyloidogenic process; the latter one being a relevant and still not well described effect in polypeptide interactions.

Authors wish to thank the financial aid received from Universidad Nacional del Litoral, Santa Fe, Argentina (CAI+D-2011) and CONICET (PIP-112-201101-00060).

The authors have declared no conflict of interest.

5 References

[1] El Rassi, Z., *Electrophoresis* 2010, *31*, 174–191.
[2] Kašička, V., *Electrophoresis* 2010, *31*, 122–146.
[3] Kašička, V., *Electrophoresis* 2012, *33*, 48–73.

[4] Selvaraju, S., El Rassi, Z., *Electrophoresis* 2012, *33*, 74–88.

[5] Righetti, P. G., Sebastiano, R., Citterio, A., *Proteomics* 2013, *13*, 325–340.

[6] Kašička, V., *Electrophoresis* 2014, *34*, 69–95.

[7] Šolínová, V., Kašička, V., Koval, D., Hlaváček, J., *Electrophoresis* 2004, *25*, 2299–2308.

[8] Piaggio, M. V., Peirotti, M. B., Deiber, J. A., *Electrophoresis* 2005, *26*, 3232–3246.

[9] Simó, C., González, R., Barbas, C., Cifuentes, A., *Anal. Chem.* 2005, *77*, 7709–7716.

[10] Benavente, F., Balaguer, E., Barbosa, J., Sanz-Nebot, V., *J. Chromatogr. A* 2006, *1117*, 94–102.

[11] Xin, Y., Mitchell, H., Cameron, H., Allison, S. A., *J. Phys. Chem. B* 2006, *110*, 1038–1045.

[12] Piaggio, M. V., Peirotti, M. B., Deiber, J. A., *Electrophoresis* 2006, *27*, 4631–4647.

[13] Piaggio, M. V., Peirotti, M. B., Deiber, J. A., *Electrophoresis* 2007, *28*, 2223–2234.

[14] Šolínová, V., Kašička, V., Sázelová, P., Barth, T., Mikšík, I., *J. Chromatogr. A* 2007, *1155*, 146–153.

[15] Piaggio, M. V., Peirotti, M. B., Deiber, J. A., *Electrophoresis* 2007, *28*, 3658–3673.

[16] Pei, H., Xin, Y., Allison, S. A., *J. Sep. Sci.* 2008, *31*, 555–564.

[17] Peirotti, M. B., Piaggio, M. V., Deiber, J. A., *J. Sep. Sci.* 2008, *31*, 548–554.

[18] Piaggio, M. V., Peirotti, M. B., Deiber, J. A., *Electrophoresis* 2009, *30*, 2328–2336.

[19] Pei, H., Allison, S., *J. Chromatogr. A*. 2009, *1216*, 1908–1916.

[20] Piaggio, M. V., Peirotti, M. B., Deiber, J. A., *J. Sep. Sci.* 2010, *33*, 2423–2429.

[21] Allison, S. A., Pei, H., Allen, M., Brown, J., Chang-II, K., Zhen, Y., *J. Sep. Sci.* 2010, *33*, 2439–2446.

[22] Deiber, J. A., Piaggio, M. V., Peirotti, M. B., *Electrophoresis* 2011, *32*, 2779–2787.

[23] Allison, S. A., Perrin, C., Cottet, H., *Electrophoresis* 2011, *32*, 2788–2796.

[24] Wu, H. F., Allison, S. A., Perrin, C., Cottet, H., *J. Sep., Sci.* 2012, *35*, 556–562.

[25] Deiber, J. A., Piaggio, M. V., Peirotti, M. B., *Electrophoresis* 2012, *33*, 990–999.

[26] Deiber, J. A., Piaggio, M. V., Peirotti, M. B., *Electrophoresis* 2013, *34*, 700–707.

[27] Deiber, J. A., Piaggio, M. V., Peirotti, M. B., *Electrophoresis* 2013, *34*, 708–715.

[28] Deiber, J. A., Piaggio, M. V., Peirotti, M. B., *Electrophoresis* 2013, *34*, 2648–2654.

[29] Deiber, J. A., Piaggio, M. V., Peirotti, M. B., *Electrophoresis* 2014, *35*, 755–761.

[30] Blennow, K., Hampel, H., Weiner, M., Zetterberg, H., *Nat. Rev. Neurol.* 2010, *6*, 131–144.

[31] Selkoe, D. J., *Cold Spring Harb. Perspect. Biol.* 2011, *3*, a004457.

[32] Masters, C. L., Selkoe, D. J., *Cold Spring Harb. Perspect. Med.* 2012, *2*, a006262.

[33] Inoue, K., Hosaka, D., Mochizuki, N., Akatsu, H., Tsutsumiuchi, K., Hashizume, Y., Matsukawa, N., Yamamoto, T., Toyo'oka, T., *Anal. Chem.* 2014, *86*, 797–804.

[34] Mohamed, A., Cortez, L., Posse de Chaves, E., *Current Protein and Peptide Science* 2011, *12*, 235–257.

[35] Verpillot, R., Otto, M., Klafki, H., Taverna, M., *J. Chromatogr. A* 2008, *1214*, 157–164.

[36] Cecchini, M., Curcio, R., Pappalardo, M., Melki, R., Caflisch, A., *J. Mol. Biol.* 2006, *357*, 1306–1321.

[37] Yan, Y., Wang, Ch., *J. Mol. Biol.* 2006, *364*, 853–862.

[38] Pauwels, K., Williams, T. L., Morris, K. L., Jonckheere, W., Vandersteen, A., Kelly, G., Schymkowitz, J., Rousseau, F., Pastore, A., Serpell, L. C., Broersen, K., *J. Biol. Chem.* 2012, *287*, 5650–5660.

[39] Sabella, S., Quaglia, M., Lanni, C., Racchi, M., Govoni, S., Caccialanza, G., Calligaro, A., Bellotti, V., De Lorenzi, E., *Electrophoresis* 2004, *25*, 3186–3194.

[40] Kato, M., Kinoshita, H., Enokita, M., Hori, Y., Hashimoto, T., Iwatsubo, T., Toyo'oka, T., *Anal. Chem.* 2007, *79*, 4887–4891.

[41] Colombo, R., Carotti, A., Catto, M., Racchi, M., Lanni, C., Verga, L., Caccialanza, G., De Lorenzi, E., *Electrophoresis* 2009, *30*, 1418–1429.

[42] Picou, R. A., Moses, J. P., Wellman, A. D., Kheterpal, I., Gilman, S. D., *Analyst (Cambridge, United Kingdom)* 2010, *135*, 1631–1635.

[43] Picou, R. A., Kheterpal, I., Wellman, A. D., Minnamreddy, M., Ku, G., Gilman, S. D., *J. Chromatogr. B* 2011, *879*, 627–632.

[44] Verpillot, R., Esselmann, H., Mohamadi, M. R., Klafki, H., Poirier, F., Lehnert, S., Otto, M., Wiltfang, J., Viovy, J. L., Taverna, M., *Anal. Chem.* 2011, *83*, 1696–1703.

[45] Pryor, N. E., Moss, M. A., Hestekin, Ch. N., *Int. J. Mol. Sci.* 2012, *13*, 3038–3072.

[46] von Smoluchowski, M., *Z. Phys. Chem.* 1917, *92*, 129–168.

[47] Russell, W. B., Saville, D. A., Schowalter, W. R., *Colloidal Dispersions*, Cambridge University Press, Cambridge, UK 1989.

[48] Verzola, B., Fogolari, F., Righetti, P. G., *Electrophoresis* 2001, *22*, 3728–3735.

[49] Israelachvili, J., *Intermolecular and Surface Forces*, Academic Press, London 1995.

[50] Derjaguin, B. V., Landau, L., *Acta Physicochim.* 1941, *14*, 633–662.

[51] Verwey, E. J. W., Overbeek, J. Th. G., *Theory of Stability of Lyophobic Colloids*, Elsevier Publishing Company, New York 1948.

